Am J Physiol Lung Cell Mol Physiol 309: L593–L604, 2015.
First published July 10, 2015; doi:10.1152/ajplung.00029.2015.

Activation of the nuclear factor-κB pathway during postnatal lung inflammation preserves alveolarization by suppressing macrophage inflammatory protein-2

Yanli Hou,[1] Min Liu,[1] Cristiana Husted,[1,2] Chihhsin Chen,[1] Kavitha Thiagarajan,[1] Jennifer L. Johns,[3] Shailaja P. Rao,[1] and Cristina M. Alvira[1,1]

[1]*Division of Critical Care Medicine, Department of Pediatrics, Stanford University School of Medicine, Stanford, California;* [2]*Department of Biochemistry, Faculty of Medicine, University of Nevada/Reno, Reno, Nevada; and* [3]*Department of Comparative Medicine, Stanford University School of Medicine, Stanford, California*

Submitted 26 January 2015; accepted in final form 6 July 2015

Hou Y, Liu M, Husted C, Chen C, Thiagarajan K, Johns JL, Rao SP, Alvira CM. Activation of the nuclear factor-κB pathway during postnatal lung inflammation preserves alveolarization by suppressing macrophage inflammatory protein-2. *Am J Physiol Lung Cell Mol Physiol* 309: L593–L604, 2015. First published July 10, 2015; doi:10.1152/ajplung.00029.2015.—A significant portion of lung development is completed postnatally during alveolarization, rendering the immature lung vulnerable to inflammatory stimuli that can disrupt lung structure and function. Although the NF-κB pathway has well-recognized pro-inflammatory functions, novel anti-inflammatory and developmental roles for NF-κB have recently been described. Thus, to determine how NF-κB modulates alveolarization during inflammation, we exposed *postnatal day 6* mice to vehicle (PBS), systemic lipopolysaccharide (LPS), or the combination of LPS and the global NF-κB pathway inhibitor BAY 11-7082 (LPS + BAY). LPS impaired alveolarization, decreased lung cell proliferation, and reduced epithelial growth factor expression. BAY exaggerated these detrimental effects of LPS, further suppressing proliferation and disrupting pulmonary angiogenesis, an essential component of alveolarization. The more severe pathology induced by LPS + BAY was associated with marked increases in lung and plasma levels of macrophage inflammatory protein-2 (MIP-2). Experiments using primary neonatal pulmonary endothelial cells (PEC) demonstrated that MIP-2 directly impaired neonatal PEC migration in vitro; and neutralization of MIP-2 in vivo preserved lung cell proliferation and pulmonary angiogenesis and prevented the more severe alveolar disruption induced by the combined treatment of LPS + BAY. Taken together, these studies demonstrate a key anti-inflammatory function of the NF-κB pathway in the early alveolar lung that functions to mitigate the detrimental effects of inflammation on pulmonary angiogenesis and alveolarization. Furthermore, these data suggest that neutralization of MIP-2 may represent a novel therapeutic target that could be beneficial in preserving lung growth in premature infants exposed to inflammatory stress.

bronchopulmonary dysplasia; proliferation; angiogenesis; endothelial migration

IN CONTRAST WITH OTHER organs, the lung completes a significant portion of its development immediately before and after birth. During this stage of alveolarization, division of the alveolar ducts into alveolar sacs by secondary septation and expansion of the pulmonary capillary bed via angiogenesis increase the gas exchange surface area of the lung by 20-fold (22). However, postnatal completion of growth renders the lung highly susceptible to environmental insults that disrupt this developmental program. This is particularly evident in the setting of preterm birth, where disruption of alveolarization causes bronchopulmonary dysplasia (BPD), a chronic lung disease associated with significant morbidity during infancy (5, 34) and a higher risk for the development of future lung diseases during adulthood (20, 71).

Inflammation is detrimental to the developing lung. Mechanical ventilation and hyperoxia, stimuli that induce lung inflammation, impair alveolarization. Preterm infants with a history of maternal chorioamnionitis are at increased risk for developing BPD (69), and intra-amniotic administration of lipopolysaccharide (LPS) impairs alveolar and vascular growth in animal models (63, 70). In addition, infants with very low birth weight and a history of either early or late-onset sepsis have an increased incidence of BPD (19, 35). However, although growing evidence supports the notion that inflammation impairs alveolarization, the molecular mechanisms responsible for these detrimental effects on distal lung growth and the endogenous pathways invoked to preserve lung growth during inflammatory stress are not known.

The NF-κB signaling pathway is a key regulator of inflammation. NF-κB molecules, although ubiquitously expressed (52), are normally held inactive in the cytoplasm in association with an inhibitory protein, IκB. Activation of NF-κB by IKK-α and -β results in the phosphorylation and degradation of IκB (50), thereby allowing NF-κB complexes to translocate into the nucleus. NF-κB-mediated induction of cytokines and chemokines has been implicated in the pathobiology of lung diseases marked by excessive inflammation (23, 39), including acute lung injury, asthma, and cystic fibrosis (10, 13, 18). However, NF-κB also serves essential anti-inflammatory functions that are cell and stimulus specific. In a rodent model of carrageenan-induced pleurisy, prophylactic inhibition of NF-κB before injury decreases inflammation, whereas inhibition after injury prolongs the inflammatory response (37). Epithelial-specific deletion of IKK-β limits lung inflammation in adult mice infected with group B streptococcus (GBS), yet macrophage-specific deletion augments inflammation by increasing signal transducer and activator of transcription (STAT)1 activation and polarizing macrophages toward the pro-inflammatory M1 phenotype (21).

Moreover, the pro- and anti-inflammatory roles of NF-κB in the lung appear to be developmentally regulated. Our group showed that systemic blockade of the NF-κB pathway in adult

Address for reprint requests and other correspondence: C. M. Alvira, Stanford Univ. School of Medicine, Center for Excellence in Pulmonary Biology, 770 Welch Road, Suite 350, Stanford, CA 94305-5162 (e-mail: calvira@stanford.edu).

mice protects against LPS-induced lung injury, whereas the same treatment worsens lung inflammation in *postnatal day 6* (P6) mice (2). In addition, we have recently demonstrated that NF-κB plays an essential role in mediating alveolarization (21). NF-κB is constitutively active in the lungs of mice at the onset of alveolarization, and pharmacologic inhibition of the NF-κB pathway at this stage of development disrupts alveolarization and reduces pulmonary capillary density, but has no effect on the lung structure of adult mice. Thus when NF-κB plays a detrimental or protective role in the developing lung remains incompletely understood.

In this study we demonstrated that systemic inflammation impairs alveolarization, decreasing lung cell proliferation and reducing epithelial growth factor expression. Inhibiting the NF-κB pathway markedly exaggerated the detrimental effects of systemic LPS on alveolarization, disrupting pulmonary angiogenesis and further suppressing proliferation. These effects were associated with an augmentation of the lung inflammatory response, as evidenced by increased STAT-1 activation and marked elevations in the levels of macrophage inflammatory protein-2 (MIP-2). Finally, MIP-2 was found to have a direct anti-migratory effect on the pulmonary endothelial cells, and neutralization of MIP-2 prevented the severe phenotype induced by NF-κB pathway inhibition, restoring both lung cell proliferation and pulmonary angiogenesis.

MATERIALS AND METHODS

Animal model. P6 C57BL/6 mice were injected intraperitoneally with vehicle (PBS), E.Coli O127:B8 LPS (24 mEU/kg; Sigma-Aldrich, St. Louis, MO), or the selective IKK-α and IKK-β inhibitor BAY 11-7082 (BAY; 10 mg/kg; EMD Chemicals, Gibbstown, NJ), 1 h before LPS. For each litter, approximately one third of the pups randomly received PBS, LPS, or LPS + BAY. For the MIP-2 neutralization experiments, four litters of pups were mixed and received either isotype control rat IgG (10 μg/g) or rat anti-mouse MIP-2 antibody (10 μg/g) (R&D systems, Minneapolis, MN). After 16 h, the IgG or anti-MIP-2 pretreated pups were then given either LPS or LPS + BAY as described above. In both sets of studies, the mice were euthanized 24 h after treatment (at *day P7*), and the lungs were fixed at 25 cm H_2O pressure with 10% formalin and paraffin was embedded for histology as we have done previously. Additional animals were also euthanized on P6 and the lungs inflation fixed as described above to allow the baseline assessment of radial alveolar counts in the mice before intervention. Morphometric analysis was performed on lung sections after formalin fixation (described above). Brightfield images of hematoxylin and eosin (H&E)-stained lung tissue were acquired using a Leica DM5500 upright microscope and a Micropublisher 5MPixel, color digital camera, using HC Plan Apo 25-mm objectives at ×10 and ×20 magnification (Leica Microsystems, Buffalo Grove, IL). Radial alveolar counts were determined in a minimum of 30 perpendicular lines per animal derived from three lung sections per animal and averaged to give a single value per mouse, as previously described (32). The area of all complete distal air spaces (nonbranching, terminal air spaces with complete circumferential walls) were measured using a 10× calibrated objective and Metamorph image analysis software, as previously described (12). For each experiment, 5 to 8 animals per group were used.

Frozen sections of lung were obtained 24 h after treatment by inflation of the lungs with optimal cutting temperature (OCT) compound embedding medium (Sakura Finetek, Torrance, CA) at a pressure of 35 cm H_2O pressure (due to the high viscosity), then immersed in OCT and snap-frozen before cryosectioning. Additional neonatal lungs were snap-frozen at 8 and 24 h for RNA and protein isolation. All animal procedures were approved by the Institutional Animal Care and Use Committee at Stanford University.

Immunofluorescent staining of lung tissue. Immunohistochemistry was performed on formalin-fixed or frozen lung sections using techniques previously described (32) with primary antibodies against proliferating cell nuclear antigen (PCNA; 1:150; Abcam, Cambridge, MA), CD31 (1:200 for frozen tissue; BD Pharmingen, San Diego, CA; or 1:200 for fixed tissue: Dianova, Germany), fibroblast growth factor-7 (FGF-7; 1:100; Santa Cruz Biotechnology, Santa Cruz, CA), fibroblast growth factor-10 (FGF-10; 1:100; Santa Cruz Biotechnology), von Willebrand factor (vWF; 1:100; Millipore, Billerica, MA), MIP-2 (1:100; R&D systems), and Ly-6B (1:100; AbD Serotec, Kidlington, UK). After being probed with the primary antibody, sections were washed in PBS for 3 × 10 min and then incubated with the suitable fluorochrome-labeled secondary antibodies (1:200; Invitrogen/Molecular Probes). Chromatin was counterstained with 10 mg/ml Hoechst reagent (Sigma-Aldrich) diluted in H_2O (1:10,000). TUNEL staining was performed using the ApoTag Peroxidase In Situ kit (Millipore), as we have done previously (2).

The PCNA-stained nuclear area relative to all nuclear area was determined in >20 nonoverlapping, random fields, derived from 5 to 6 animals per group, and the value of the total PCNA-stained nuclear area was divided by the Hoechst-stained nuclear area after thresholding. The values were then averaged to derive a single value of percent PCNA-stained nuclear area for each animal. The number of vWF positive vessels (diameter <100 μm) per high-powered field (HPF) was manually counted on 20× images in a blinded fashion. At least 10 nonoverlapping fields per mouse were counted, and the number of vWF positive vessels per HPF averaged to give a single value per mouse. The number of lung neutrophils and TUNEL positive cells present in each group was quantified in four nonoverlapping 20× images in a blinded fashion, with the number of neutrophils or TUNEL positive cells per HPF averaged to give a single value per mouse.

Western immunoblot. Cytoplasmic and nuclear protein was extracted from frozen lung tissue using the NE-PER kit (Pierce), quantified using the Bradford method, and then subjected to SDS-PAGE. Membranes were incubated with primary antibodies to detect either VEGF-A (Abcam; 1:500) or VEGFR2 (Santa Cruz Biotechnology; 1:500) with α-tubulin (Sigma; 1:5,000) as a loading control, cleaved-caspase-3 (Cell Signaling; 1:500) with β-actin as a loading control, and p-STAT1 (Cell Signaling; 1:1,000) with TATA box binding protein (TBP; Abcam; 1:2,000) as a loading control. For the in vitro studies to assess activation of STAT-1, murine alveolar macrophage (MH-S) cells and pulmonary endothelial cells (PEC) were pretreated with BAY 11-7082 (5 μM) for 1 h, followed by stimulation with LPS (100 ng/ml) for 4 h, and nuclear protein was extracted, subjected to SDS-PAGE, and probed to detect p-STAT1 with the nuclear envelope protein Lamin-B1 (Abcam; 1:5,000) The appropriate horseradish peroxidase-conjugated secondary antibody, were used to detect the immune-complexes as enhanced chemiluminescence signals on Kodak X-ray films (GE Life Sciences, Piscataway, NJ). Images of the Western blot were processed by use of the ImageJ software.

Quantification of MIP-2 in plasma. Neonatal plasma was collected using plasma separator tubes (BD, Franklin Lakes, NJ). The plasma levels of MIP-2 were quantified using a MIP-2 ELISA kit (R&D Systems) performed according to the manufacturer's protocol.

Isolation of PECs. Neonatal primary PEC were isolated after digestion of whole lung tissue with collagenase IA (0.5 mg/ml) for 30 min at 37°C and incubation of cell homogenate for 15 min at room temperature (RT) with anti-CD31 coated magnetic beads (Dynabeads, Invitrogen) as previously described (24). PEC were cultured in endothelial growth media (EGM) containing 5% FBS (Microvascular EBM-2; Lonza) at 37°C in 5% CO_2. Cells from passages 1 through 3 were used for all experiments.

Proliferation assays. Proliferation of neonatal PEC was determined by performing bromodeoxyuridine (BrdU) incorporation assays. PEC (6K) were plated in each well (96-well plate) and allowed to attach in EGM for 24 h. After 12 h of starvation in EGM + 0.2% serum, the media was replaced with starvation media containing vehicle (PBS + 1% BSA) or increasing concentrations of recombinant murine MIP-2 (R&D Systems) in addition to BrdU. The BrdU incorporation was measured at 4 to 72 h post-treatment by ELISA per the manufacturer's protocol (Roche Diagnostics, Mannheim, Germany).

Endothelial wound healing assays. Migration of neonatal PEC was determined by wound healing assay. PEC (6K) were plated on culture slides and allowed to attach in EGM for 24 h. A linear wound was created using a sterile pipet tip, and the EGM media was then replaced with either starvation or complete (EGM + 5% serum) media containing either vehicle (PBS + 1% BSA) or increasing concentrations of recombinant MIP-2 (R&D Systems). Phase-contrast images of the wound were obtained at 0 and 16 h post-treatment, and the percentage of the wound area covered at 16 h calculated in at least three wells for each experimental group.

Apoptosis assays. To assess apoptosis, 10K PEC were plated into each well of a 96-well plate and allowed to attach for 24 h in complete EGM. At time zero, EGM was replaced with starvation media containing vehicle (PBS + 1% BSA) or increasing concentrations of recombinant MIP-2, and the amount of cleaved caspase-3 and -7 was measured using a GloMax 96-well plate luminometer and the Caspase Glo-3/7 reagent (Promega) at 2 to 8 h.

Statistical analyses. All data are presented as means ± SE. Statistical differences between two groups were determined by Student's *t*-test and between more than two groups by one-way ANOVA, followed by Bonferroni Multiple Comparison post hoc analysis. Statistical differences between groups where there were two independent variables were determined using two-way ANOVA. A P value of ≤ 0.05 was considered statistically significant.

RESULTS

Systemic LPS disrupts distal growth of the early alveolar lung and, inhibiting the NF-κB pathway, accentuates these detrimental effects. Clinical and experimental studies have shown that antenatal inflammation detrimentally affects alveolarization; however, the role of postnatal systemic inflammation on the early alveolar lung is less clear. To investigate whether systemic inflammation alters late lung development, we treated mice at the onset of alveolarization (6-day-old; P6) with a sublethal dose of systemic LPS and assessed lung structure at 24 h post-treatment. Systemic LPS impaired alveolarization in the neonatal mouse, increasing the distal airspace size by more than 30% ($P < 0.001$; Fig. 1*B*) and reducing radial alveolar counts by 20% ($P < 0.001$; Fig. 1*C*) as compared with vehicle controls (PBS).

To determine the effect of NF-κB pathway activation on alveolarization during systemic inflammation, we then treated additional groups of LPS-treated mice with BAY-11-7082, a selective and irreversible inhibitor of IKK-α and -β (51). Our previous study demonstrated that BAY treatment alone,- impaired alveolarization in P6 mice, resulting in a 20% decrease in the radial alveolar count (RAC) and a similar increase in distal airspace size (21). In keeping with these results, inhibiting the NF-κB pathway with BAY exaggerated the alveolar simplification induced by systemic LPS, with LPS + BAY mice demonstrating a 30% decrease in RAC and a 40% increase in distal airspace size (Fig. 1, *B* and *C*) than mice receiving LPS alone. To assess whether the decreased alveolarization observed in the LPS and LPS + BAY groups represented primarily an arrest in the formation of new alveoli versus the active destruction of existing alveoli, RAC were also determined in P6 mice at baseline. The RAC of LPS-treated mice at P7 and control mice at P6 were similar (5.52 ± 0.06 vs. 5.53 ± 0.16, ns). In contrast, the RAC in LPS + BAY-treated mice at P7 were significantly less than control mice at P6 (4.2 ± 0.02 vs. 5.52 ± 0.06; $p < 0.001$), suggesting that the combination of LPS + BAY causes destruction of existing alveoli in addition to inducing arrested alveolar development.

Systemic LPS reduces proliferation and decreases epithelial growth factors in the early alveolar lung. We next evaluated the effect of systemic inflammation, in the presence or absence of NF-κB pathway inhibition, on lung cell apoptosis and proliferation. We first assessed the amount of apoptosis in the

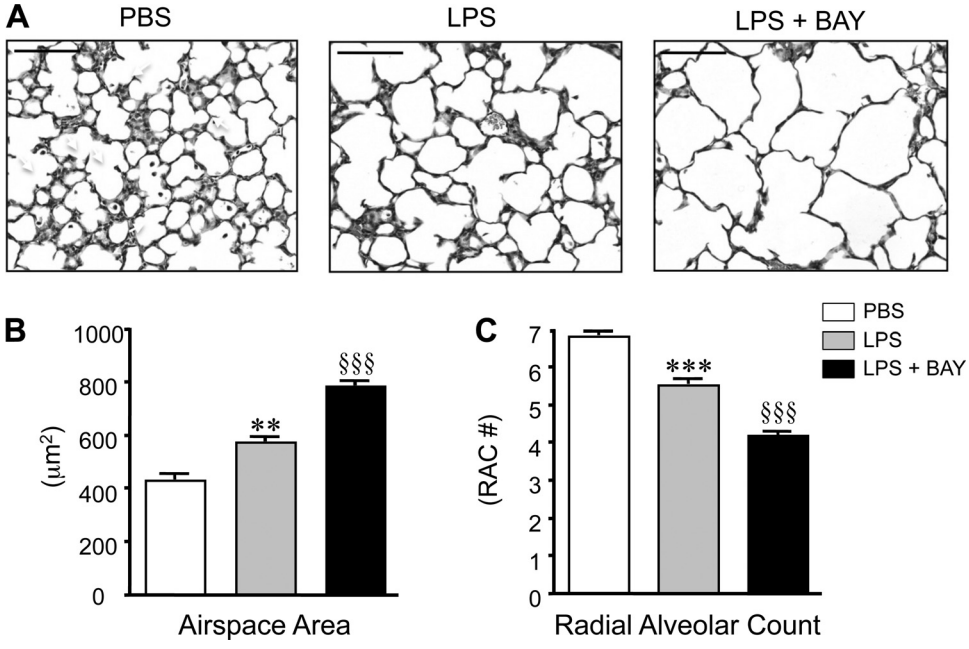

Fig. 1. Systemic lipopolysaccharide (LPS) disrupts distal lung growth in the early alveolar lung, and inhibiting the NF-κB pathway accentuates these detrimental effects. *A*: representative images of hematoxylin and eosin (H&E)-stained lung sections obtained from *postnatal day 7* (P7) mice, 24 h after administration of vehicle (PBS), LPS, or LPS + BAY 11-7082 (LPS + BAY). *B*: morphometric analysis to determine the distal airspace area, with $^{**}P < 0.01$ vs. PBS and §§§$P < 0.001$ vs. PBS and LPS. *C*: morphometric analysis to determine the radial alveolar count, with $^{***}P < 0.001$ vs. PBS and §§§$P < 0.001$ vs. PBS and LPS. All data are expressed as means ± SE, with $n = 6$–9 animals per group. Scale bar = 100 μm. RAC, radial alveolar count.

lungs of PBS, LPS, and LPS + BAY-treated mice at 8 h by determining the amount of cleaved caspase-3 by Western immunoblot. We found a strong trend toward similarly increased levels of cleaved caspase-3 in the lungs of LPS and LPS + BAY-treated mice, but these were not statistically different than controls (Fig. 2*A*). We also did not detect significant differences in the amount of apoptosis between the three groups by TUNEL staining of lung sections at 24 h (1.7 ± 0.45, 3.3 ± 1, and 4 ± 0.67 TUNEL positive cells per HPF in PBS, LPS, and LPS + BAY-treated mice, respectively, with $n = 5$).

To assess the degree of proliferation, we immunostained fixed lung tissue from the three groups of mice to detect PCNA. Consistent with prior reports, a high rate of proliferating cells was found throughout the lungs of control mice (Fig. 2*B*). Systemic LPS reduced proliferation in the early alveolar lung, resulting in a 60% decrease in PCNA nuclear staining in LPS-treated versus control mice ($P < 0.01$; Fig. 2*C*). Inhibiting the NF-κB pathway further decreased proliferation in the early alveolar lung, with mice receiving the combination of LPS + BAY demonstrating an 80% reduction as compared with that of controls ($P < 0.001$).

We next determined whether the decreased proliferation observed in the LPS and LPS + BAY-treated mice was associated with alterations in the expression of key epithelial growth factors FGF-7 and FGF-10. We first determined the gene expression of FGF-7 and FGF-10 in the three groups of mice, 8 h after treatment with PBS, BAY, LPS, or LPS + BAY, using quantitative PCR. BAY treatment alone did not change the gene expression of either FGF-7 or FGF-10 (data not shown). In contrast, systemic LPS decreased the mRNA expression of both FGF-7 and FGF-10 (Fig. 2, *D* and *E*). However, NF-κB pathway inhibition did not further reduce FGF-7 and FGF-10 levels in the LPS-treated mice. These decreases in FGF-7 and FGF-10 mRNA expression correlated with the immunostaining of lung sections to detect FGF-7 and FGF-10 protein in situ, which showed similar reductions in FGF-7 and FGF-10 protein in both the LPS and the LPS + BAY-treated mice (Fig. 2*F*).

Systemic LPS disrupts pulmonary angiogenesis and decreases the expression of angiogenic factors and, inhibiting the NF-κB pathway, accentuates these effects. Growth of the pulmonary capillaries by angiogenesis is essential for alveolarization. However, how systemic inflammation alters pulmonary capillary development, and whether activation of NF-κB in this setting is beneficial or detrimental, has not been studied. Therefore, to determine the pulmonary capillary density in the three groups of mice, we immunostained lung sections with an antibody against the endothelial cell marker CD31. Previously, we demonstrated that BAY treatment alone reduced CD31 immunoreactivity by 24 h (21). Similarly, LPS treatment resulted in a modest reduction in CD31 immunostaining, and

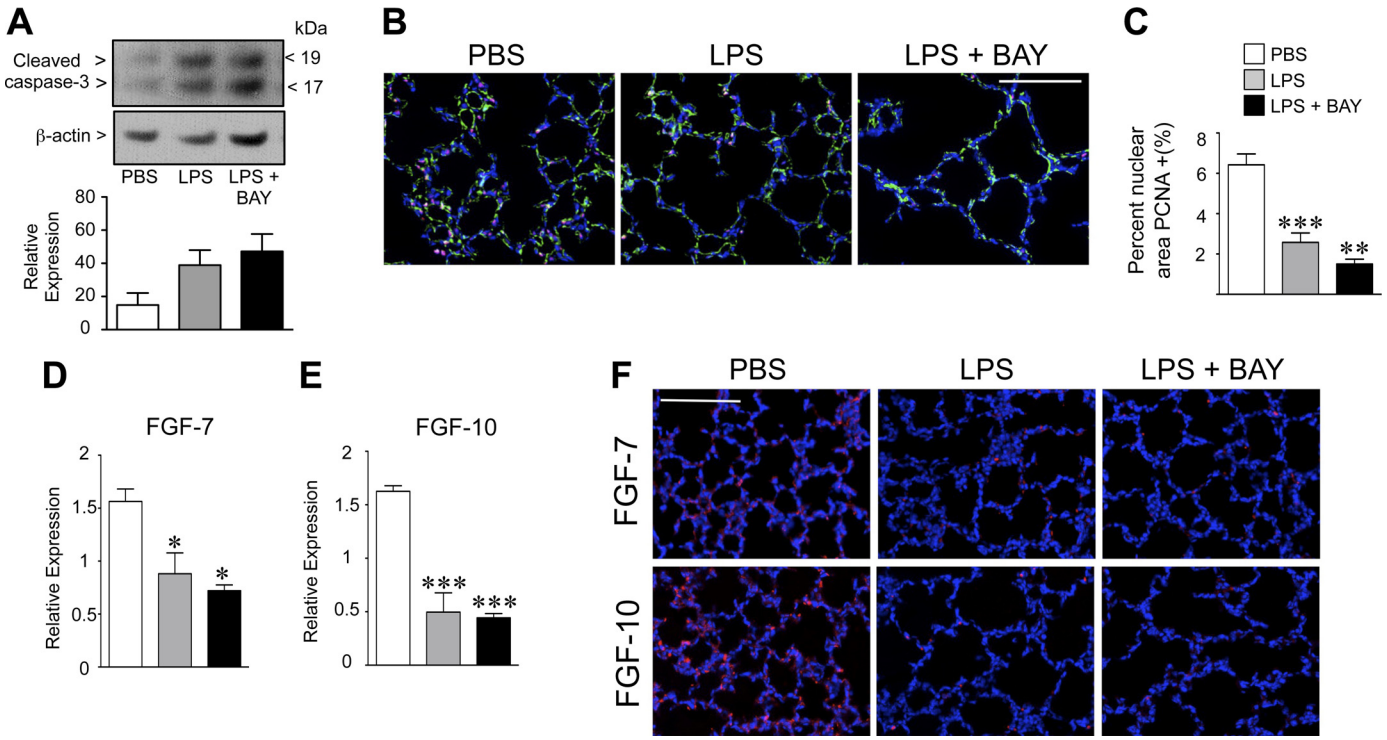

Fig. 2. Systemic LPS reduces proliferation and decreases epithelial growth factors in the early alveolar lung. *A*: Western immunoblot to detect cleaved-caspase 3 in lung tissue from PBS, LPS, and LPS + BAY-treated mice at 8 h. Data are expressed as means ± SE, with $n = 4$ to 5 for each group. *B*: representative composite immunofluorescent images from lung frozen sections obtained from PBS, LPS, and LPS + BAY-treated neonatal mice at 24 h, to detect p65 (red), CD31 (green), and chromatin (blue). Scale bar = 100 μm. *C*: quantification of the proliferating cell nuclear antigen (PCNA) positive nuclear area in the lungs of each group, with $^{**}P < 0.01$ and $^{***}P < 0.001$ vs. PBS. Data are expressed as means ± SE, with $n = 5$ to 6 for each group. *D*: quantitative RT-PCR performed on whole lung, 8 h after either administration of PBS, LPS, or LPS + BAY to detect fibroblast growth factor (FGF)-7 and FGF-10 (*E*), with $^{*}P < 0.05$ and $^{***}P < 0.001$ vs. PBS. Data are expressed as means ± SE, with $n = 4$ for each group. *F*: representative composite immunofluorescent images from lung frozen sections obtained from PBS, LPS, and LPS + BAY-treated neonatal mice at 24 h to detect either FGF-7 or FGF-10 (red) and chromatin (blue). Scale bar = 100 μm.

combined treatment with LPS + BAY resulted in more marked reductions (Fig. 3*A*). We further evaluated these differences in pulmonary vascular density by immunostaining lung sections to detect vWF and quantifying the number of microvessels per HPF (61, 65). Systemic LPS treatment resulted in a small but statistically insignificant decrease in vessel density, whereas LPS + BAY reduced the number of small blood vessels by 30% (Fig. 3*C*).

The VEGF signaling pathway is a key regulator of the pulmonary angiogenesis requisite for alveolarization. To determine whether systemic inflammation impairs alveolarization by disrupting VEGF signaling, we quantified the protein expression of VEGF-A and VEGFR-2 in PBS, LPS, and LPS + BAY-treated neonatal mouse lung. Lung levels of VEGFR2 protein were markedly decreased in response to systemic LPS, and inhibiting the NF-κB pathway did not further suppress VEGFR2 expression. In contrast, although VEGF-A protein was similar in the lungs of LPS-treated mice as compared with those of PBS controls (Fig. 3*E*), VEGF-A protein expression was significantly less in LPS + BAY-treated mice. These results suggest that the more severe impairment in alveolarization observed in the LPS + BAY-treated mice may result in part from disrupted pulmonary angiogenesis.

Inhibiting the NF-κB pathway in the early alveolar lung enhances activation of STAT-1 and increases LPS-mediated inflammation. Classically considered a pro-inflammatory mediator, NF-κB also serves essential anti-inflammatory functions that are cell and stimulus specific (1). For example, in macrophages, loss of IKK-β increases STAT-1 activation, augmenting inflammatory cytokine expression by polarizing macrophages toward an M1, pro-inflammatory phenotype (21). To determine whether BAY treatment altered STAT1 in the signaling of the three groups of mice, we immunostained frozen lung tissue to detect phosphorylated (active) STAT-1. Lung sections from PBS-treated mice were completely devoid of pSTAT-1 positive cells (Fig. 4*A*). Systemic LPS activated STAT1 in the early alveolar mouse lung, evident by the nuclear staining of scattered, isolated cells for pSTAT1 in the lungs of mice receiving LPS alone, including cells that were CD31 positive (arrows). Inhibiting the NF-κB pathway further in-

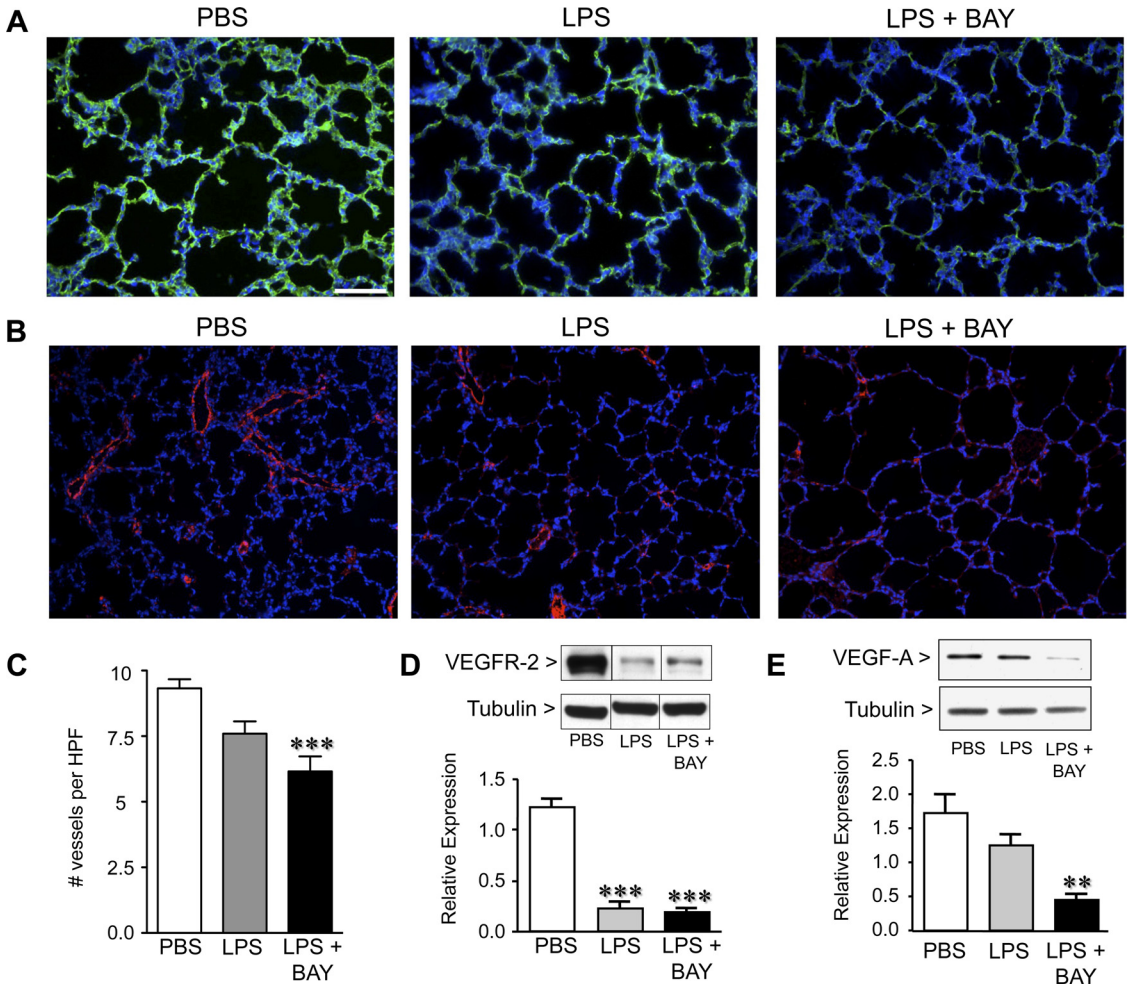

Fig. 3. Systemic LPS disrupts pulmonary angiogenesis and decreases the expression of angiogenic factors, and inhibiting the NF-κB pathway accentuates these effects. *A*: representative immunofluorescent images from lung frozen sections obtained from PBS, LPS, and LPS + BAY-treated mice at 24 h, to detect CD31 (green) and chromatin (blue) (*A*) or von Willebrand factor (vWF; red) and chromatin (blue) (*B*). *C*: quantification of vWF-stained vessels per high power field (HPF) in each group with $***P < 0.001$ vs. PBS. Data are expressed as means ± SE, with $n = 5$ to 6 for each group. *D*: Western immunoblot to detect VEGFR-2 and VEGF-A (*E*) in lung tissue from PBS, LPS, and LPS + BAY-treated mice at 24 h, and normalized to tubulin as a loading control, with $**P < 0.01$ and $***P < 0.001$ vs. PBS. Dividing lines between bands on the VEGFR2 WB indicate that the bands were from the same gel, but not from adjacent wells. Data are expressed as means ± SE, with $n = 4$ for each group. Scale bar = 100 μm.

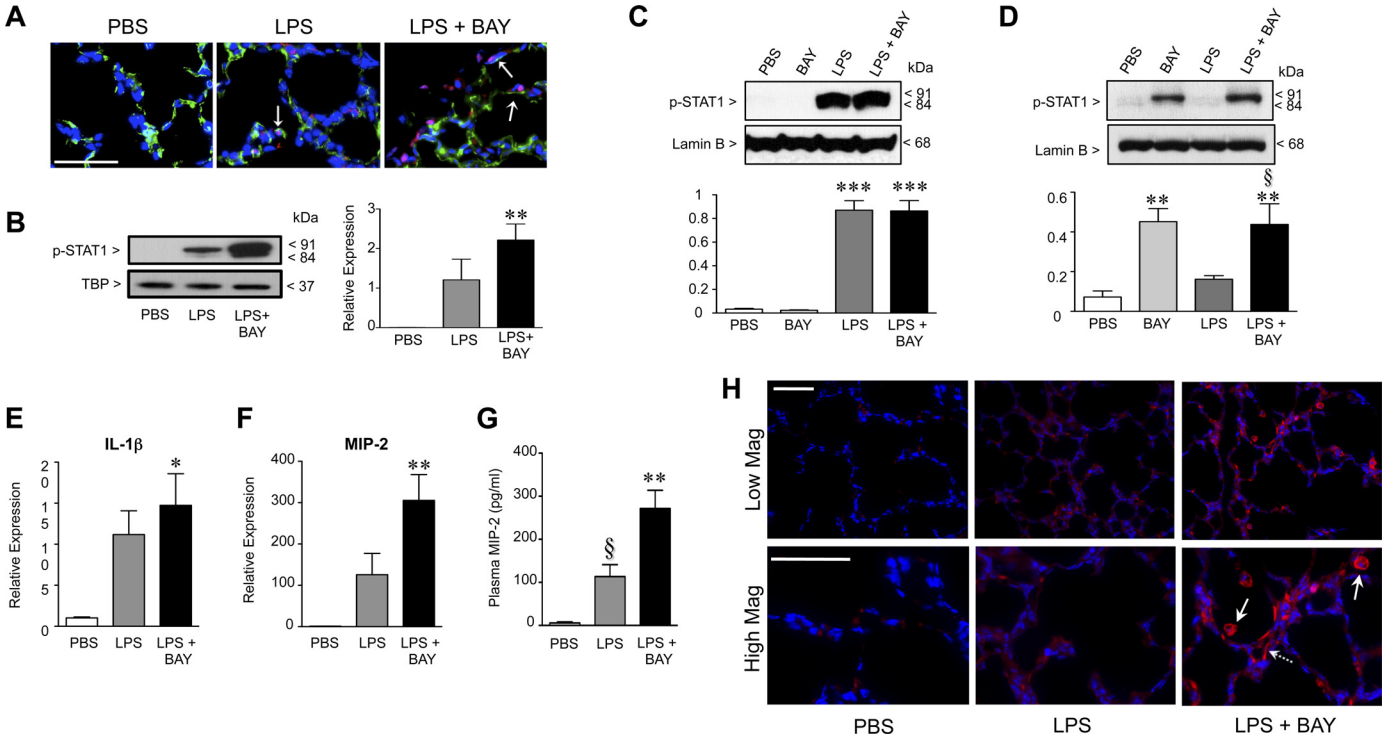

Fig. 4. Inhibiting the NF-κB pathway in the early alveolar lung enhances activation of signal transducer and activator of transcription (STAT)-1 and increases LPS-mediated inflammation. *A*: representative immunofluorescent images of lung frozen sections obtained from PBS, LPS, and LPS + BAY-treated mice at 8 h, to detect CD31 (green), p-STAT1 (red), and chromatin (blue). Arrows indicated cells that are CD31 positive and contain nuclear pSTAT-1. *B*: Western immunoblot to detect p-STAT-1 protein in nuclear extracts obtained from lungs of PBS, LPS, and LPS + BAY-treated neonatal mice at 8 h and normalized to TATA-box binding protein (TBP) as a loading control with $^{**}P < 0.01$ vs. PBS ($n = 4$ for each group). Data are expressed as means ± SE, with $n = 4$ for each group. *C*: Western immunoblot to detect p-STAT-1 protein in nuclear extracts obtained from murine alveolar macrophage (MH-S) or primary pulmonary endothelial cells (*D*) pretreated with BAY (5 μM) for 1 h before stimulation with LPS (100 ng/ml) for 4 h and normalized to the nuclear envelope protein lamin-B1. $^{***}P < 0.001$ vs. PBS for *C* and $^{**}P < 0.01$ vs. PBS and $\S P < 0.05$ vs. LPS (*D*), with data combined from $n = 4$ to 5 independent experiments. *E*: quantitative RT-PCR to detect the mRNA expression of IL-1β and macrophage inflammatory protein (MIP)-2 (*F*) in lung tissue from PBS, LPS, and LPS + BAY-treated neonatal mice at 8 h, with $^{*}P < 0.05$ and $^{**}P < 0.01$ vs. PBS. Data are expressed as means ± SE, with $n = 4$ for each group. *G*: ELISA to determine the concentration of MIP-2 in plasma samples obtained from PBS, LPS, and LPS + BAY-treated neonatal mice at 24 h, with $^{**}P < 0.01$ vs. PBS and $\S P < 0.05$ vs. LPS + BAY. Data are expressed as means ± SE, with $n = 5$–13 for each group. *H*: representative images of immunofluorescence stained lung frozen sections obtained from PBS, LPS, and LPS + BAY-treated neonatal mice at 24 h at low (*top*) and high (*bottom*) magnification (Mag), to detect MIP-2 (red) and chromatin (blue). Scale bars = 50 μm.

creased STAT-1 activation, with lungs from LPS + BAY-treated mice demonstrating numerous cells with intense nuclear staining for pSTAT1. These differences were quantified by immunoblot analysis using nuclear extracts obtained from whole lung tissue, which showed a nonsignificant increase in nuclear pSTAT1 in LPS-treated mice and a more marked, statistically significant increase in the lungs of mice treated with LPS + BAY (Fig. 4*B*).

In both macrophages and endothelial cells, LPS can induce STAT1 activation (41, 56). Thus, to evaluate how the NF-κB pathway modulates STAT1 activation in these two cell types, we next performed in vitro studies in alveolar macrophages and primary pulmonary endothelial cells exposed to LPS. Murine alveolar macrophages (MH-S cells) were pretreated with BAY for 1 h before stimulation with LPS, and nuclear protein assessed for STAT-1 activation at 4 h. LPS activated STAT1 in the MH-S cells, and the degree of activation was completely unaffected by pretreatment with BAY (Fig. 4*C*). In contrast, LPS alone did not activate STAT1 in primary PEC, but the combination of LPS + BAY significantly induced STAT1 activation (Fig. 4*D*). Furthermore, treating the MH-S cells with BAY alone had no effect on STAT-1 activation, whereas BAY alone increased STAT-1 activation in PEC. Taken together, these data suggest that in our in vivo model, the increased STAT-1 activation observed may be occurring primarily in the pulmonary endothelium rather than in alveolar macrophages.

In addition to STAT-1 being activated, systemic LPS also increased the gene expression of inflammatory factors that have been implicated in other models of impaired alveolarization, including IL-1β (14) and the CXC chemokine macrophage inflammatory protein-2 (MIP-2) (40). Although BAY treatment alone did not alter the expression of these two cytokines (data not shown), inhibiting the NF-κB pathway in the LPS-treated mice raised IL-1β levels slightly (Fig. 4*E*) and markedly increased the levels of MIP-2, resulting in a 300-fold increase in MIP-2 mRNA in the LPS + BAY mice as compared with PBS controls and a 2.4-fold increase as compared with mice treated with LPS alone (Fig. 4*F*). These increases in MIP-2 mRNA expression correlated with results obtained from the immunostaining of lung sections at 24 h to detect MIP-2 protein in situ. Lung sections from PBS controls demonstrated minimal MIP-2 immunoreactivity (Fig. 4*H*), and systemic LPS modestly increased MIP-2 immunoreactivity in the lung. However, inhibiting the NF-κB pathway markedly increased MIP-2

immunoreactivity in LPS-treated animals, with intense staining evident in large cells within the alveoli (solid arrows) and in flat cells lining pulmonary capillaries (dashed arrow). Furthermore, these changes in lung MIP-2 expression were reflected by similar changes in plasma MIP-2 levels, with modest increases in the LPS-treated animals and significantly higher levels in the plasma from mice treated with LPS + BAY (Fig. 4*G*). In addition, the heightened MIP-2 expression observed in the LPS + BAY-treated mice was also associated with a significant increase in the number of neutrophils infiltrating the lung parenchyma (7 ± 2 neutrophils per HPF in PBS, 17.75 ± 2.4 in LPS, and 25.77 ± 3 in LPS + BAY, with $P < 0.01$ in LPS + BAY vs. PBS).

Neutralizing MIP-2 in the LPS-exposed lung preserves lung proliferation and angiogenesis and prevents the severe alveolar impairment induced by NF-κB pathway inhibition. Signaling through the CXC receptor-2 (CXCR2) mediates inflammation in experimental models of lung injury induced by LPS, infection, and mechanical stretch (7, 54). However, many CXCR2 ligands, including MIP-2, also possess potent pro-angiogenic effects (58), thus raising the possibility that the heightened MIP-2 levels in the LPS + BAY animals represent a compensatory response aimed to restore pulmonary angiogenesis. Thus, to determine whether MIP-2 was playing a pathologic or compensatory role in our model, we performed experiments to neutralize MIP-2 in vivo. Groups of mice were pretreated with either anti-MIP-2 neutralizing antibody (anti-MIP-2-Ab) or isotype control antibody (IgG) before receiving either LPS or LPS + BAY. Morphometric analysis of IgG and anti-MIP-2-Ab-treated mice demonstrated that MIP-2 neutralization prevented the severe impairment of alveolarization induced by LPS + BAY (Fig. 5, *A–C*). Although treatment with anti-MIP-2-Ab did not improve alveolarization in mice treated with LPS alone, mice receiving anti-MIP-2-Ab before LPS + BAY had significantly smaller terminal airspaces (Fig. 5*B*) and increased radial alveolar counts (Fig. 5*C*) than mice treated with isotype control IgG, resulting in values that were similar to those observed in mice treated with LPS alone.

Moreover, neutralization of MIP-2 preserved lung cell proliferation and pulmonary angiogenesis in the LPS + BAY-treated mice. Quantification of PCNA positive nuclei in lung sections obtained from LPS + BAY mice treated with either IgG or anti-MIP-2-Ab demonstrated a 40% increase in the number of proliferating cells within the lung (Fig. 6*A*). Furthermore, neutralization of MIP-2 also significantly increased the pulmonary capillary density, resulting in 30% greater vWF positive vessels in the LPS + BAY mice treated with the anti-MIP-2 Ab as compared with those mice receiving IgG (Fig. 6*B*).

MIP-2 directly impairs PEC migration. The ability of the anti-MIP-2-Ab to preserve pulmonary capillary density in the LPS + BAY-treated mice suggested that MIP-2 might directly impair pulmonary endothelial angiogenesis. Thus we next performed in vitro assays to determine how MIP-2 alters key angiogenic functions of the pulmonary endothelial cells. We exposed the PEC to increasing doses of recombinant murine MIP-2 and performed assays to assess survival, proliferation, and migration. Recombinant MIP-2 did not affect PEC proliferation or survival, even at doses as high as 1 μg/ml (data not shown). In contrast, recombinant MIP-2 impaired PEC migration, with the highest concentration of MIP-2 (1 μg/ml) resulting in a 40% decrease in endothelial wound closure (Fig. 7*A*). Of note, the anti-migratory effect of MIP-2 was only observed when added to the complete media, with neither a pro- nor anti-migratory effect observed when recombinant MIP-2 was added to starvation media (Fig. 7*B*).

DISCUSSION

In the present report, we explored the role of the NF-κB pathway in the early alveolar lung during systemic inflammation. As a central regulator of inflammation, the NF-κB pathway has been shown to promote lung injury in numerous models (16, 26, 57). However, important anti-inflammatory functions for NF-κB have recently been established, and we have previously shown that constitutive activation of NF-κB promotes pulmonary angiogenesis and alveolarization (32). In this study, we found that systemic LPS alone was sufficient to disrupt alveolarization, significantly decreasing lung cell proliferation and the expression of epithelial growth factors. Ab-

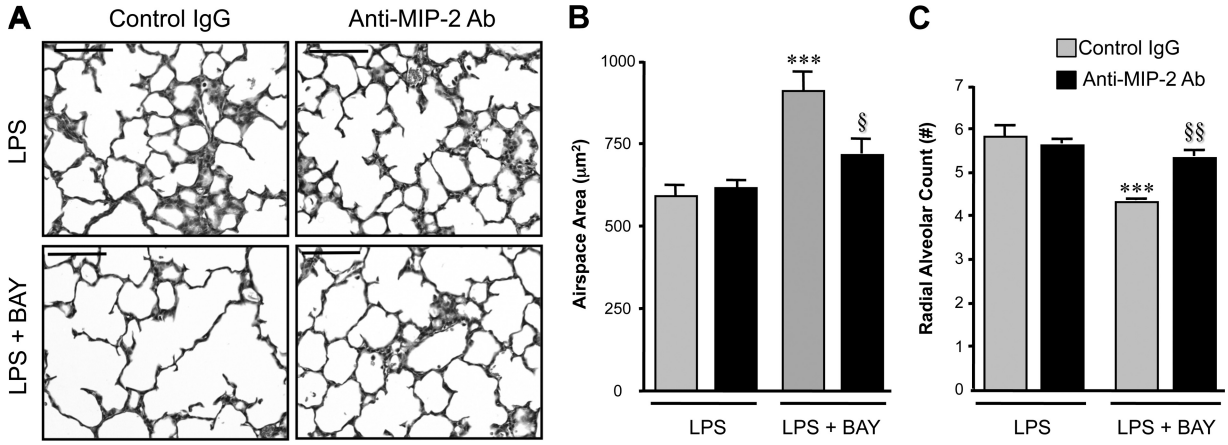

Fig. 5. MIP-2 neutralization prevents the severe disruption of alveolarization induced by inhibiting the NF-κB pathway in the LPS-exposed lung. *A*: representative images of H&E-stained lung sections from neonatal mice pretreated with either control IgG or anti-MIP-2 Ab, obtained 24 h after administration of LPS or LPS + BAY. Scale bar = 100 μm. *B*: morphometric analysis to determine the distal airspace area, with ***$P < 0.01$ vs. LPS + IgG and §$P < 0.05$ vs. LPS + BAY + IgG. Data are expressed as means ± SE, with $n = 5–7$ for each group. *C*: morphometric analysis to determine the radial alveolar count, with ***$P < 0.01$ vs. LPS + IgG and §§$P < 0.01$ vs. LPS + BAY + IgG. Data are expressed as means ± SE, with $n = 6–8$ for each group.

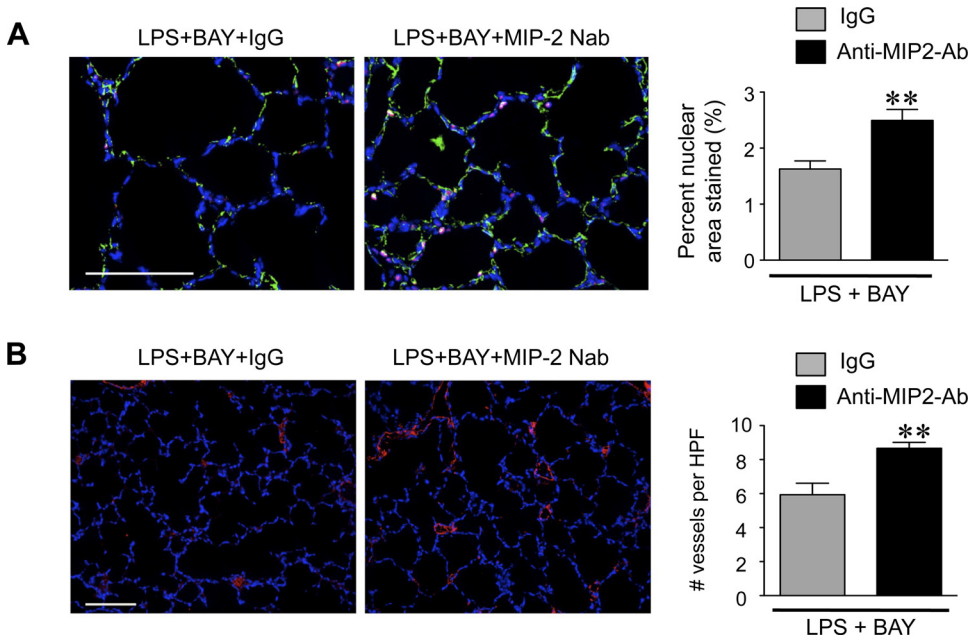

Fig. 6. MIP-2 neutralization prevents the suppressed proliferation and angiogenesis induced by inhibiting the NF-κB pathway in the LPS-exposed lung. *A*: representative immunofluorescent images of lung frozen sections from neonatal mice pretreated with either control IgG or anti-MIP-2 Ab, obtained 24 h after administration of LPS or LPS + BAY, stained to detect CD31 (green), PCNA (red), and chromatin (blue). The percent PCNA-stained nuclear to total nuclear area was calculated, with $^{**}P = 0.007$ vs. LPS + BAY + IgG. Data are expressed as means ± SE, with $n = 5$ to 6 for each group. *B*: representative immunofluorescent images of lung frozen sections from neonatal mice pretreated with either control IgG or anti-MIP-2 Ab, obtained 24 h after administration of LPS or LPS + BAY, stained to detect vWF (red) and chromatin (blue). The number of vWF-positive vessels per HPF was calculated with $^{**}P = 0.006$ vs. LPS + BAY + IgG. Data are expressed as means ± SE, with $n = 5$ to 6 for each group. Scale bar = 100 μm.

rogating the NF-κB pathway markedly exaggerated the detrimental effects of LPS on the early alveolar lung, further decreasing cell proliferation, impairing pulmonary angiogenesis, and augmenting lung inflammation, with marked increases in the CXC chemokine MIP-2. Importantly, neutralizing MIP-2 in the mice receiving both LPS and the NF-κB inhibitor BAY prevented the severe impairment in alveolarization and preserved proliferation and angiogenesis at levels observed in mice receiving LPS alone. By exploring the direct effects of MIP-2 on PEC, we related this rescue effect to the ability of MIP-2 to impair PEC migration. Taken together our data suggest that activation of NF-κB in the early alveolar lung during systemic inflammation preserves angiogenesis and alveolarization by suppressing the anti-angiogenic cytokine MIP-2.

The onset of alveolarization is characterized by a period of rapid cellular proliferation, and stimuli that disrupt alveolarization (e.g., hyperoxia and dexamethasone) reduce proliferation in the developing lung (17, 42). FGF-7 is an epithelial specific mitogen that promotes the proliferation of alveolar epithelial cells, in vitro (48) and in vivo (64). The structurally similar growth factor FGF-10 also promotes the proliferation of lung epithelial cells (49) and is essential for lung development, with FGF-10 null mice, demonstrating a complete absence of lung formation (45). In this study, we found that systemic LPS significantly decreased proliferation in the early

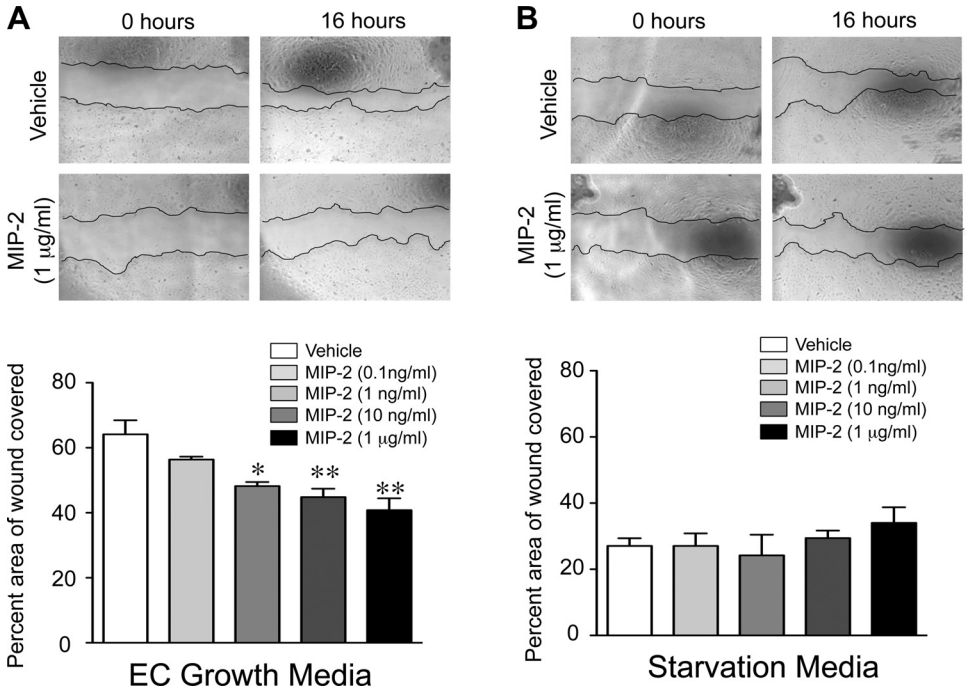

Fig. 7. MIP-2 directly impairs pulmonary endothelial cell (PEC) migration. Representative phase contrast images of wound made in confluent monolayers of neonatal primary PEC at time 0 h and 16 h, after incubation with vehicle or increasing concentrations of recombinant MIP-2 in endothelial growth media (*A*) or starvation media (*B*), are shown. The percent area of the wound covered at 16 h was quantified, with $^{*}P < 0.05$ and $^{**}P < 0.01$ vs. vehicle. Data are expressed as means ± SE, with $n = 3$ for each group.

alveolar lung and suppressed the expression of both FGF-7 and FGF-10. Although we have previously shown that blocking NF-κB in the early alveolar mouse lung suppresses lung cell proliferation (21), blocking NF-κB in the LPS-treated lung did not further suppress proliferation or decrease FGF-7 or FGF-10 expression to a greater degree than LPS alone. Thus, although LPS-mediated decreases in lung cell proliferation likely contribute to the impaired alveolarization induced by systemic inflammation, these data suggest that an alternate mechanism is responsible for the more severe phenotype observed in the LPS + BAY-treated mice.

The radial alveolar counts of mice receiving the combined treatment of LPS + BAY were significantly lower at 24 h after treatment (i.e., at *postnatal day 7*) than the radial alveolar counts of control animals at P6. These data suggest that blocking NF-κB activity during systemic inflammation does not simply arrest the formation of new alveoli but results in the destruction of existing alveoli. Although there was a strong trend toward both increased cleaved caspase-3 protein levels and number of TUNEL positive cells per HPF within the lungs of the LPS + BAY-treated mice, this did not reach statistical significance. It is possible that the absence of a statistically significant increase in these metrics represents a type II error, given the large variability present within the two treatment groups, or that the timepoints selected for these assays did not coincide with the timing of peak apoptosis in this model. Alternatively, it could be that the lung injury occurring in the LPS + BAY-treated mice resulted primarily from an induction of necrotic, rather than apoptotic, cell death. In addition, although RAC remains a very commonly used surrogate to assess lung complexity during late development (3, 27, 30, 43, 68), the application of unbiased, designed-based stereologic methods to accurately measure alveolar number would be important in future studies to more definitively determine the degree of alveolar loss in the LPS + BAY-treated mice.

Growth of the pulmonary capillaries by angiogenesis is essential for alveolarization. Angiogenic factors normally increase during late lung development but are suppressed by injuries that disrupt alveolarization (29), and pulmonary capillary density and angiogenic mediators are decreased in patients dying from BPD (9). Our prior work demonstrated that constitutive activation of NF-κB in the early alveolar lung promotes pulmonary angiogenesis (21), in part by functioning as a direct transcriptional regulator of VEGFR2 in early alveolar pulmonary endothelial cells (32). In this study we found that systemic LPS markedly decreased VEGFR2 protein in the lung and that NF-κB inhibition did not suppress VEGFR2 expression further. However, VEGF-A levels were only decreased in the mice receiving the combination of LPS and the NF-κB inhibitor. VEGF contains NF-κB binding sites within its promoter, and NF-κB has been shown to induce VEGF transcription in alveolar epithelial cells in other models (62). In concert with our findings, ATII-mediated deletion of IKK-β induces a transient impairment in alveolarization and significantly decreases VEGF expression, confirming that NF-κB regulates VEGF expression during late lung development. The combined reduction in VEGFR2 and VEGF-A in the mice treated with the combination of systemic LPS and the NF-κB inhibitor was associated with a significant decrease in pulmonary capillary density. Taken together, these data suggest that suppression of pulmonary angiogenesis is key to the severe pathology observed in the mice treated with LPS + BAY.

In keeping with our prior study (2), inhibiting the NF-κB pathway before the administration of LPS increased lung inflammation, resulting in greater neutrophilic infiltration of the lung and a marked up regulation in MIP-2. However, other studies examining the effect of NF-κB pathway inhibition on lung growth and injury have yielded conflicting results. In contrast with our findings in the early alveolar lung, in fetal lung explants from the late canalicular/early saccular stage of development, blocking NF-κB activation in macrophages ameliorates the LPS-induced disruption of airway branching (11). Similarly, inhibiting the NF-κB pathway with BAY decreases lung cytokine expression in LPS-treated adult mice (2). Yet, pretreatment of 6-wk-old mice with dexamethasone before LPS administration potently inhibits NF-κB pathway activation and increases lung neutrophil accumulation and MIP-2 production (4), similar to what we observed in the present study. Mice containing compound genetic deletions of NF-κB subunits develop spontaneous inflammation, increased neutrophils, and heightened levels of CXC chemokines (67). However, although epithelial-specific deletion of IKK-β limits lung inflammation in adult mice infected with GBS, macrophage-specific deletion of IKK-β augments inflammation by polarizing macrophages toward a pro-inflammatory phenotype (21). Furthermore, partial inhibition of IKK-β activity decreases inflammation and injury in a lung transplant model, whereas complete inhibition of IKK-β significantly exaggerates lung inflammation (31). Taken together, these studies highlight the complexity of NF-κB signaling in the lung and suggest that the effects of blocking the NF-κB pathway will vary depending on the timing, degree, and cell-specificity of the inhibition. In addition, both IKK-α and IKK-β have recently been described to possess NF-κB-independent functions (15), suggesting that distinct effects might be observed using strategies to directly block IKK activity (as done in this study using BAY), versus those that specifically target NF-κB nuclear translocation.

In our model, a key feature of the pathology induced by the combined treatment of LPS + BAY was the marked upregulation of the pro-inflammatory chemokine MIP-2. However, the mechanisms accounting for this MIP-2 overexpression remain unclear. Important anti-inflammatory functions of NF-κB result from its ability to regulate macrophage polarization. Activation of macrophages to the M1 phenotype by bacterial products such as LPS induces the expression of inflammatory cytokines (8) and angiostatic chemokines (47), whereas activation to the M2 phenotype enhances tissue repair by promoting cell growth, extracellular matrix remodeling (66), and angiogenesis (via the induction of VEGF-A). The NF-κB pathway regulates both the switch from the M1 to the M2 phenotype and also the pro-angiogenic function of M2 macrophages. Monocyte-specific deletion of IKK-β increases M1 polarization by abrogating IKK-β-mediated inhibition of STAT1, a transcriptional regulator of M1 cytokines (21). Similarly, survival of M1 macrophages is prolonged in mice with an inactive form of IKK-α (36). NF-κB enhances the formation of collateral vessels after ischemia by increasing the accumulation of M2 macrophages (60) and is necessary for maintaining the M2-phenotype of tumor associated macrophages (25).

In our model, inhibition of NF-κB significantly increased STAT1 in the LPS-exposed lung, and although a portion of these cells were CD31 positive EC, there were other cell types within the lung that also activated STAT1. However, our in vitro experiments performed in macrophages and EC (two cell types known to activate STAT1 in response to LPS) demonstrated that BAY did not alter STAT-1 activation in LPS-stimulated alveolar macrophages but enhanced STAT-1 activation in LPS-stimulated PEC. Of note, treating the pulmonary endothelial cells with BAY alone also resulted in a marked increase in STAT1 activation, suggesting that NF-κB serves to suppress STAT1 activity even under control conditions. These data suggest that the heightened cytokine production may be originating from the pulmonary endothelium rather than the alveolar macrophages. However, additional studies will be necessary to definitively identify all of the specific cellular sources of activated STAT1 in the lung and to determine whether it is these same cells that are specifically producing MIP-2. Future studies aimed to establish whether systemic inhibition of NF-κB polarizes the alveolar macrophages toward an M1 phenotype would also be important to determine whether alterations in macrophage polarization could explain both the increased MIP-2 and decreased VEGF-A observed in our model. Moreover, additional studies to explore whether inhibiting NF-κB in LPS-exposed lung differentially activates transcription factors (e.g., p38 MAPK, JNK) and cytokines (e.g., TNF-α) known to regulate MIP-2 would be important to further delineate the mechanisms leading to MIP-2 overexpression.

The CXC/CXCR2 axis modulates lung injury in other models. CXC chemokines such as MIP-2 recruit neutrophils into the lung during acute inflammation (53). In an experimental model of acute viral infection, anti-CXCR2 antibodies preserve alveolarization and decrease neutrophil accumulation (40). Similarly, $CXCR2^{-/-}$ mice exposed to hyperoxia demonstrate decreased lung infiltration and improved survival as compared with controls (59). Furthermore, in an inflammatory model of BPD induced by the overexpression of IL-1β during the saccular stage of lung development, loss of CXCR2 attenuated the detrimental effects of IL-1β on alveolarization (28). The combined treatment of LPS + BAY increased lung neutrophils, and it is not possible to differentiate whether the beneficial effects of MIP-2 neutralization were primarily related to the inhibition of neutrophil accumulation versus the inhibition of direct MIP-2 effects on the pulmonary endothelium. However, evidence suggests that neutrophils promote angiogenesis, in part, by secreting high levels of angiogenic factors such as VEGF (33). In our model, the severe alveolar impairment in the mice receiving LPS + BAY was associated with both decreased angiogenesis and lower levels of VEGF, suggesting that mechanisms, in addition to neutrophilic infiltration, are central to the pathology.

In the present report, we identified a novel, anti-migratory effect of MIP-2 on the PEC. This is in contrast with data demonstrating that MIP-2 and additional ELR+ CXC cytokines promote migration and angiogenesis in other endothelial cell types (58). However, varied angiogenic responses of endothelial cells in response to CXC cytokines have been described. Human dermal microvascular EC have a more potent chemotactic response toward the CXC chemokine, IL-8, than human umbilical vein EC due to differences in the expression of distinct CXC receptors between the two cells types (55). In contradistinction, EC chemotaxis is greater in murine aortic EC than in pulmonary EC, despite similar levels of expression of the MIP-2 receptor CXCR2 (46). Of note, in that study by Moldobaeva and Wagner (46), there was a strong trend toward impaired migration in lung microvascular EC treated with the highest dose of MIP-2 (100 ng/ml). In our studies, the anti-migratory effects of MIP-2 on the primary PEC were only observed when MIP-2 was added to endothelial growth media containing serum. These data suggest that MIP-2 may block pro-angiogenic pathways mediated by endothelial growth factors present in serum. Alternatively, given that CXCR2 has numerous ligands, the detrimental effect of MIP-2 on pulmonary angiogenesis could be the result of high levels of MIP-2 serving to sequester CXCR2 from other, pro-angiogenic ligands. This notion may explain why the modest elevations of MIP-2 observed in the mice treated with LPS alone do not appear to be detrimental and why the neutralization of MIP-2 in that group had no effect on lung structure. Moreover, our data that plasma MIP-2 levels mirror the induction of MIP-2 in the lung raise the possibility that levels above a certain threshold might identify patients that would benefit from MIP-2 neutralization to preserve alveolarization, particularly in the subgroup of patients that develop postnatal infections.

In this study, we used a potent, pharmacologic inhibitor of the IKK kinases BAY 11-7082. Although this strategy had the advantage of completely blocking both IKK-α and-β phosphorylation, it remains possible that BAY may have influenced other intracellular signaling pathways in addition to NF-κB. Furthermore, inhibiting NF-κB activation with BAY did not allow us to differentiate whether the beneficial effects are mediated through IKK-α or IKK-β or to determine whether these IKK-mediated benefits are NF-κB dependent. Moreover, because BAY would inhibit IKK activity in all cell types, this strategy did not permit us to delineate the cell type responsible for the protective effect. Abrogation of NF-κB signaling via genetic deletion of either p65 or IKK-β causes embryonic lethality at E15.5 (6, 38), precluding the use of these ubiquitous knockout models to study pathology occurring later in development. Our in vitro studies suggest that the increased STAT-1 activation observed in the neonatal mice exposed to LPS + BAY may be the result of heightened STAT-1 phosphorylation in the PEC. Moving forward, the creation of a murine model with an inducible, endothelial specific deletion of IKK-β would allow the definitive assessment of the unique contribution of endothelial-specific activation of NF-κB to alveolarization during physiologic and pathologic conditions.

In conclusion, the present study highlights an important role for the NF-κB pathway in preserving pulmonary angiogenesis and alveolarization during postnatal inflammation. This is an extension of our prior studies, which demonstrated a novel anti-inflammatory role of NF-κB in the early alveolar lung and identified an essential function for constitutive activation of the NF-κB pathway in alveolarization and angiogenesis. These data identify a central role for NF-κB in mitigating the detrimental effects of inflammation on alveolarization by suppressing MIP-2 expression and suggest that clinical studies in infants to correlate plasma MIP-2 levels with the severity of lung injury could potentially identify a subgroup of patients who might benefit from MIP-2 neutralization as a therapy to preserve lung growth. In addition, our work adds to a growing

body of evidence derived from our group and others (2, 32, 44, 72), supporting a unique, beneficial role for NF-κB during late lung development and specific, physiologic roles for NF-κB in the pulmonary endothelium. Moving forward, the challenge will be to further delineate the mechanisms that control the distinct functions of NF-κB, to tailor the development of therapeutic strategies to selectively enhance discrete components of the pathway to effectively treat or prevent lung diseases such as BPD.

GRANTS

This work was supported by National Heart, Lung, and Blood Institute Grants 1P30HL-101315-01 (to C. M. Alvira) and R01 HL-122918-01 (to C. M. Alvira) and the American Heart Association Fellow to Faculty Award 0875001N (to C. M. Alvira).

DISCLOSURES

No conflicts of interest, financial or otherwise are declared by the author(s).

AUTHOR CONTRIBUTIONS

Author contributions: Y.H. and C.M.A. conception and design of research; Y.H., M.L., C.H., C.C., K.T., J.L.J., S.P.R., and C.M.A. performed experiments; Y.H., M.L., C.H., C.C., K.T., J.L.J., S.P.R., and C.M.A. analyzed data; Y.H., M.L., C.H., K.T., S.P.R., and C.M.A. interpreted results of experiments; Y.H., C.H., K.T., and C.M.A. edited and revised manuscript; Y.H., M.L., C.H., C.C., K.T., J.L.J., S.P.R., and C.M.A. approved final version of manuscript; C.H. and C.M.A. prepared figures; C.M.A. drafted manuscript.

REFERENCES

1. **Alvira CM.** Nuclear factor-kappa-B signaling in lung development and disease: one pathway, numerous functions. *Birth Defects Res A Clin Mol Teratol* 100: 202–216, 2014.
2. **Alvira CM, Abate A, Yang G, Dennery PA, Rabinovitch M.** Nuclear factor-kappaB activation in neonatal mouse lung protects against lipopolysaccharide-induced inflammation. *Am J Respir Crit Care Med* 175: 805–815, 2007.
3. **Ambalavanan N, Stanishevsky A, Bulger A, Halloran B, Steele C, Vohra Y, Matalon S.** Titanium oxide nanoparticle instillation induces inflammation and inhibits lung development in mice. *Am J Physiol Lung Cell Mol Physiol* 304: L152–L161, 2013.
4. **Aoki K, Ishida Y, Kikuta N, Kawai H, Kuroiwa M, Sato H.** Role of CXC chemokines in the enhancement of LPS-induced neutrophil accumulation in the lung of mice by dexamethasone. *Biochem Biophys Res Commun* 294: 1101–1108, 2002.
5. **Balinotti JE, Chakr VC, Tiller C, Kimmel R, Coates C, Kisling J, Yu Z, Nguyen J, Tepper RS.** Growth of lung parenchyma in infants and toddlers with chronic lung disease of infancy. *Am J Respir Crit Care Med* 181: 1093–1097, 2010.
6. **Beg AA, Baltimore D.** An essential role for NF-kappaB in preventing TNF-alpha-induced cell death. *Science* 274: 782–784, 1996.
7. **Belperio JA, Keane MP, Burdick MD, Londhe V, Xue YY, Li K, Phillips RJ, Strieter RM.** Critical role for CXCR2 and CXCR2 ligands during the pathogenesis of ventilator-induced lung injury. *J Clin Invest* 110: 1703–1716, 2002.
8. **Benoit M, Desnues B, Mege JL.** Macrophage polarization in bacterial infections. *J Immunol* 181: 3733–3739, 2008.
9. **Bhatt AJ, Pryhuber GS, Huyck H, Watkins RH, Metlay LA, Maniscalco WM.** Disrupted pulmonary vasculature and decreased vascular endothelial growth factor, Flt-1, and TIE-2 in human infants dying with bronchopulmonary dysplasia. *Am J Respir Crit Care Med* 164: 1971–1980, 2001.
10. **Blackwell TS, Blackwell TR, Holden EP, Christman BW, Christman JW.** In vivo antioxidant treatment suppresses nuclear factor-kappa B activation and neutrophilic lung inflammation. *J Immunol* 157: 1630–1637, 1996.
11. **Blackwell TS, Hipps AN, Yamamoto Y, Han W, Barham WJ, Ostrowski MC, Yull FE, Prince LS.** NF-kappaB signaling in fetal lung macrophages disrupts airway morphogenesis. *J Immunol* 187: 2740–2747, 2011.
12. **Bland RD, Mokres LM, Ertsey R, Jacobson BE, Jiang S, Rabinovitch M, Xu L, Shinwell ES, Zhang F, Beasley MA.** Mechanical ventilation with 40% oxygen reduces pulmonary expression of genes that regulate lung development and impairs alveolar septation in newborn mice. *Am J Physiol Lung Cell Mol Physiol* 293: L1099–L1110, 2007.
13. **Brouillard F, Bouthier M, Leclerc T, Clement A, Baudouin-Legros M, Edelman A.** NF-kappa B mediates up-regulation of CFTR gene expression in Calu-3 cells by interleukin-1beta. *J Biol Chem* 276: 9486–9491, 2001.
14. **Bry K, Whitsett JA, Lappalainen U.** IL-1beta disrupts postnatal lung morphogenesis in the mouse. *Am J Respir Cell Mol Biol* 36: 32–42, 2007.
15. **Chariot A.** The NF-kappaB-independent functions of IKK subunits in immunity and cancer. *Trends Cell Biol* 19: 404–413, 2009.
16. **Cheng DS, Han W, Chen SM, Sherrill TP, Chont M, Park GY, Sheller JR, Polosukhin VV, Christman JW, Yull FE, Blackwell TS.** Airway epithelium controls lung inflammation and injury through the NF-kappa B pathway. *J Immunol* 178: 6504–6513, 2007.
17. **Clement A, Edeas M, Chadelat K, Brody JS.** Inhibition of lung epithelial cell proliferation by hyperoxia. *Posttranscriptional regulation of proliferation-related genes J Clin Invest* 90: 1812–1818, 1992.
18. **Everhart MB, Han W, Sherrill TP, Arutiunov M, Polosukhin VV, Burke JR, Sadikot RT, Christman JW, Yull FE, Blackwell TS.** Duration and intensity of NF-kappaB activity determine the severity of endotoxin-induced acute lung injury. *J Immunol* 176: 4995–5005, 2006.
19. **Fanaroff AA, Korones SB, Wright LL, Verter J, Poland RL, Bauer CR, Tyson JE, Philips JB, 3rd Edwards W, Lucey JF, Catz CS, Shankaran S, Oh W.** Incidence, presenting features, risk factors and significance of late onset septicemia in very low birth weight infants. *The National Institute of Child Health and Human Development Neonatal Research Network Pediatr Infect Dis J* 17: 593–598, 1998.
20. **Fawke J, Lum S, Kirkby J, Hennessy E, Marlow N, Rowell V, Thomas S, Stocks J.** Lung function and respiratory symptoms at 11 years in children born extremely preterm: the EPICure study. *Am J Respir Crit Care Med* 182: 237–245, 2010.
21. **Fong CH, Bebien M, Didierlaurent A, Nebauer R, Hussell T, Broide D, Karin M, Lawrence T.** An antiinflammatory role for IKKbeta through the inhibition of "classical" macrophage activation. *J Exp Med* 205: 1269–1276, 2008.
22. **Galambos C, Demello DE.** Regulation of alveologenesis: clinical implications of impaired growth. *Pathology* 40: 124–140, 2008.
23. **Grossmann M, Nakamura Y, Grumont R, Gerondakis S.** New insights into the roles of ReL/NF-kappa B transcription factors in immune function, hemopoiesis and human disease. *Int J Biochem Cell Biol* 31: 1209–1219, 1999.
24. **Guignabert C, Alvira CM, Alastalo TP, Sawada H, Hansmann G, Zhao M, Wang L, El-Bizri N, Rabinovitch M.** Tie2-mediated loss of peroxisome proliferator-activated receptor-gamma in mice causes PDGF receptor-beta-dependent pulmonary arterial muscularization. *Am J Physiol Lung Cell Mol Physiol* 297: L1082–L1090, 2009.
25. **Hagemann T, Lawrence T, McNeish I, Charles KA, Kulbe H, Thompson RG, Robinson SC, Balkwill FR.** "Re-educating" tumor-associated macrophages by targeting NF-kappaB. *J Exp Med* 205: 1261–1268, 2008.
26. **Hart LA, Krishnan VL, Adcock IM, Barnes PJ, Chung KF.** Activation and localization of transcription factor, nuclear factor-kappaB, in asthma. *Am J Respir Crit Care Med* 158: 1585–1592, 1998.
27. **Hilgendorff A, Parai K, Ertsey R, Navarro E, Jain N, Carandang F, Peterson J, Mokres L, Milla C, Preuss S, Alcazar MA, Khan S, Masumi J, Ferreira-Tojais N, Mujahid S, Starcher B, Rabinovitch M, Bland R.** Lung matrix and vascular remodeling in mechanically ventilated elastin haploinsufficient newborn mice. *Am J Physiol Lung Cell Mol Physiol* 308: L464–L478, 2015.
28. **Hogmalm A, Backstrom E, Bry M, Lappalainen U, Lukkarinen HP, Bry K.** Role of CXC chemokine receptor-2 in a murine model of bronchopulmonary dysplasia. *Am J Respir Cell Mol Biol* 47: 746–758, 2012.
29. **Hosford GE, Olson DM.** Effects of hyperoxia on VEGF, its receptors, and HIF-2alpha in the newborn rat lung. *Am J Physiol Lung Cell Mol Physiol* 285: L161–L168, 2003.
30. **Hou A, Fu J, Yang H, Zhu Y, Pan Y, Xu S, Xue X.** Hyperoxia stimulates the transdifferentiation of type II alveolar epithelial cells in newborn rats. *Am J Physiol Lung Cell Mol Physiol* 308: L861–L872, 2015.
31. **Huang HJ, Sugimoto S, Lai J, Okazaki M, Yamamoto S, Krupnick AS, Kreisel D, Gelman AE.** Maintenance of IKKbeta activity is neces-

sary to protect lung grafts from acute injury. *Transplantation* 91: 624–631, 2011.
32. **Iosef C, Alastalo TP, Hou Y, Chen C, Adams ES, Lyu SC, Cornfield DN, Alvira CM.** Inhibiting NF-kappaB in the developing lung disrupts angiogenesis and alveolarization. *Am J Physiol Lung Cell Mol Physiol* 302: L1023–L1036, 2012.
33. **Jablonska J, Leschner S, Westphal K, Lienenklaus S, Weiss S.** Neutrophils responsive to endogenous IFN-beta regulate tumor angiogenesis and growth in a mouse tumor model. *J Clin Invest* 120: 1151–1164, 2010.
34. **Kinsella JP, Greenough A, Abman Bronchopulmonary dysplasia SH.** *Lancet (could not determine journal name)* 367: 1421–1431, 2006.
35. **Klinger G, Levy I, Sirota L, Boyko V, Lerner-Geva L, Reichman B.** Outcome of early-onset sepsis in a national cohort of very low birth weight infants. *Pediatrics* 125: e736–740, 2010.
36. **Lawrence T, Bebien M, Liu GY, Nizet V, Karin M.** IKKalpha limits macrophage NF-kappaB activation and contributes to the resolution of inflammation. *Nature* 434: 1138–1143, 2005.
37. **Lawrence T, Gilroy DW, Colville-Nash PR, Willoughby DA.** Possible new role for NF-kappaB in the resolution of inflammation. *Nat Med* 7: 1291–1297, 2001.
38. **Li Q, Van Antwerp D, Mercurio F, Lee KF, Verma IM.** Severe liver degeneration in mice lacking the IkappaB kinase 2 gene. *Science* 284: 321–325, 1999.
39. **Liu SF, Malik AB.** NF-kappa B activation as a pathological mechanism of septic shock and inflammation. *Am J Physiol Lung Cell Mol Physiol* 290: L622–L645, 2006.
40. **Londhe VA, Belperio JA, Keane MP, Burdick MD, Xue YY, Strieter RM.** CXCR2/CXCR2 ligand biological axis impairs alveologenesis during dsRNA-induced lung inflammation in mice. *Pediatr Res* 58: 919–926, 2005.
41. **Luu K, Greenhill CJ, Majoros A, Decker T, Jenkins BJ, Mansell A.** STAT1 plays a role in TLR signal transduction and inflammatory responses. *Immunol Cell Biol* 92: 761–769, 2014.
42. **Luyet C, Burri PH, Schittny JC.** Suppression of cell proliferation and programmed cell death by dexamethasone during postnatal lung development. *Am J Physiol Lung Cell Mol Physiol* 282: L477–L483, 2002.
43. **Mandell E, Seedorf G, Gien J, Abman SH.** Vitamin D treatment improves survival and infant lung structure after intra-amniotic endotoxin exposure in rats: potential role for the prevention of bronchopulmonary dysplasia. *Am J Physiol Lung Cell Mol Physiol* 306: L420–L428, 2014.
44. **McKenna S, Michaelis KA, Agboke F, Liu T, Han K, Yang G, Dennery PA, Wright CJ.** Sustained hyperoxia-induced NF-kappaB activation improves survival and preserves lung development in neonatal mice. *Am J Physiol Lung Cell Mol Physiol* 306: L1078–L1089, 2014.
45. **Min H, Danilenko DM, Scully SA, Bolon B, Ring BD, Tarpley JE, DeRose M, Simonet WS.** Fgf-10 is required for both limb and lung development and exhibits striking functional similarity to Drosophila branchless. *Genes Dev* 12: 3156–3161, 1998.
46. **Moldobaeva A, Wagner EM.** Difference in proangiogenic potential of systemic and pulmonary endothelium: role of CXCR2. *Am J Physiol Lung Cell Mol Physiol* 288: L1117–L1123, 2005.
47. **Owen JL, Mohamadzadeh M.** Macrophages and chemokines as mediators of angiogenesis. *Front Physiol* 4: 159, 2013.
48. **Panos RJ, Rubin JS, Csaky KG, Aaronson SA, Mason RJ.** Keratinocyte growth factor and hepatocyte growth factor/scatter factor are heparin-binding growth factors for alveolar type II cells in fibroblast-conditioned medium. *J Clin Invest* 92: 969–977, 1993.
49. **Park WY, Miranda B, Lebeche D, Hashimoto G, Cardoso WV.** FGF-10 is a chemotactic factor for distal epithelial buds during lung development. *Dev Biol* 201: 125–134, 1998.
50. **Perkins ND.** Integrating cell-signalling pathways with NF-kappaB and IKK function. *Nat Rev Mol Cell Biol* 8: 49–62, 2007.
51. **Pierce JW, Schoenleber R, Jesmok G, Best J, Moore SA, Collins T, Gerritsen ME.** Novel inhibitors of cytokine-induced IkappaBalpha phosphorylation and endothelial cell adhesion molecule expression show anti-inflammatory effects in vivo. *J Biol Chem* 272: 21096–21103, 1997.
52. **Read MA, Whitley MZ, Williams AJ, Collins T.** NF-kappa B and I kappa B alpha: an inducible regulatory system in endothelial activation. *J Exp Med* 179: 503–512, 1994.
53. **Remick DG, Green LB, Newcomb DE, Garg SJ, Bolgos GL, Call DR.** CXC chemokine redundancy ensures local neutrophil recruitment during acute inflammation. *Am J Pathol* 159: 1149–1157, 2001.
54. **Reutershan J, Morris MA, Burcin TL, Smith DF, Chang D, Saprito MS, Ley K.** Critical role of endothelial CXCR2 in LPS-induced neutrophil migration into the lung. *J Clin Invest* 116: 695–702, 2006.
55. **Salcedo R, Resau JH, Halverson D, Hudson EA, Dambach M, Powell D, Wasserman K, Oppenheim JJ.** Differential expression and responsiveness of chemokine receptors (CXCR1-3) by human microvascular endothelial cells and umbilical vein endothelial cells. *FASEB J* 14: 2055–2064, 2000.
56. **Sikorski K, Chmielewski S, Przybyl L, Heemann U, Wesoly J, Baumann M, Bluyssen HA.** STAT1-mediated signal integration between IFNgamma and LPS leads to increased EC and SMC activation and monocyte adhesion. *Am J Physiol Cell Physiol* 300: C1337–C1344, 2011.
57. **Skerrett SJ, Liggitt HD, Hajjar AM, Ernst RK, Miller SI, Wilson CB.** Respiratory epithelial cells regulate lung inflammation in response to inhaled endotoxin. *Am J Physiol Lung Cell Mol Physiol* 287: L143–L152, 2004.
58. **Strieter RM, Polverini PJ, Kunkel SL, Arenberg DA, Burdick MD, Kasper J, Dzuiba J, Van Damme J, Walz A, Marriott D, Chan SY, Roczniak S, and Shanafelt.** The functional role of the ELR motif in CXC chemokine-mediated angiogenesis. *J Biol Chem* 270: 27348–27357, 1995.
59. **Sue RD, Belperio JA, Burdick MD, Murray LA, Xue YY, Dy MC, Kwon JJ, Keane MP, Strieter RM.** CXCR2 is critical to hyperoxia-induced lung injury. *J Immunol* 172: 3860–3868, 2004.
60. **Takeda Y, Costa S, Delamarre E, Roncal C, Leite de Oliveira R, Squadrito ML, Finisguerra V, Deschoemaeker S, Bruyere F, Wenes M, Hamm A, Serneels J, Magat J, Bhattacharyya T, Anisimov A, Jordan BF, Alitalo K, Maxwell P, Gallez B, Zhuang ZW, Saito Y, Simons M, De Palma M, Mazzone M.** Macrophage skewing by Phd2 haplodeficiency prevents ischaemia by inducing arteriogenesis. *Nature* 479: 122–126, 2011.
61. **Tang JR, Seedorf G, Balasubramaniam V, Maxey A, Markham N, Abman SH.** Early inhaled nitric oxide treatment decreases apoptosis of endothelial cells in neonatal rat lungs after vascular endothelial growth factor inhibition. *Am J Physiol Lung Cell Mol Physiol* 293: L1271–L1280, 2007.
62. **Tong Q, Zheng L, Lin L, Li B, Wang D, Huang C, Li D.** VEGF is upregulated by hypoxia-induced mitogenic factor via the PI-3K/Akt-NF-kappaB signaling pathway. *Respir Res* 7: 37, 2006.
63. **Ueda K, Cho K, Matsuda T, Okajima S, Uchida M, Kobayashi Y, Minakami H, Kobayashi K.** A rat model for arrest of alveolarization induced by antenatal endotoxin administration. *Pediatr Res* 59: 396–400, 2006.
64. **Ulich TR, Yi ES, Longmuir K, Yin S, Biltz R, Morris CF, Housley RM, Pierce GF.** Keratinocyte growth factor is a growth factor for type II pneumocytes in vivo. *J Clin Invest* 93: 1298–1306, 1994.
65. **Vadivel A, Alphonse RS, Collins JJ, van Haaften T, O'Reilly M, Eaton F, Thebaud B.** The axonal guidance cue semaphorin 3C contributes to alveolar growth and repair. *PLoS One* 8: e67225, 2013.
66. **Varin A, Gordon S.** Alternative activation of macrophages: immune function and cellular biology. *Immunobiology* 214: 630–641, 2009.
67. **von Vietinghoff S, Asagiri M, Azar D, Hoffmann A, Ley K.** Defective regulation of CXCR2 facilitates neutrophil release from bone marrow causing spontaneous inflammation in severely NF-kappa B-deficient mice. *J Immunol* 185: 670–678, 2010.
68. **Wang H, Jafri A, Martin RJ, Nnanabu J, Farver C, Prakash YS, MacFarlane PM.** Severity of neonatal hyperoxia determines structural and functional changes in developing mouse airway. *Am J Physiol Lung Cell Mol Physiol* 307: L295–L301, 2014.
69. **Watterberg KL, Demers LM, Scott SM, Murphy S.** Chorioamnionitis and early lung inflammation in infants in whom bronchopulmonary dysplasia develops. *Pediatrics* 97: 210–215, 1996.
70. **Willet KE, Jobe AH, Ikegami M, Newnham J, Brennan S, Sly PD.** Antenatal endotoxin and glucocorticoid effects on lung morphometry in preterm lambs. *Pediatr Res* 48: 782–788, 2000.
71. **Wong PM, Lees AN, Louw J, Lee FY, French N, Gain K, Murray CP, Wilson A, Chambers DC.** Emphysema in young adult survivors of moderate-to-severe bronchopulmonary dysplasia. *Eur Respir J* 32: 321–328, 2008.
72. **Yang G, Abate A, George AG, Weng YH, Dennery PA.** Maturational differences in lung NF-kappaB activation and their role in tolerance to hyperoxia. *J Clin Invest* 114: 669–678, 2004.